SLAC-PUB-2294
March 1979
(T/E)

EXCLUSIVE PROCESSES AND THE EXCLUSIVE-INCLUSIVE CONNECTION IN QUANTUM CHROMODYNAMICS

Stanley J. Brodsky*
Stanford Linear Accelerator Center
Stanford University, Stanford, California 94305

and

G. Peter Lepage**
Laboratory of Nuclear Studies
Cornell University, Ithaca, New York 14853

1. Introduction

Although the structure of large momentum transfer inclusive reactions is now well understood in perturbative quantum chromodynamics, exclusive processes involving large transfer of momentum have received relatively little attention since they involve detailed, explicit features of hadronic wavefunctions. On the other hand, the dimensional counting[1,2] ansatz, which is based on the premise that the high momentum tail of wavefunctions can be computed from the first iteration of a scale-invariant Bethe-Salpeter kernel, leads to a number of successful predictions for form factors, hadron scattering and photoproduction at large angles, as well as the $x \to 1$ dependence of the structure functions.

In brief, the dimensional counting rules are:

(a) (Spin-averaged) form factors at $|t| \gg M^2$ (Fig. 1a)

$$F_H(t) \sim \frac{1}{t^{n-1}} \tag{1.1}$$

where n = number of constituent fields in H.

(b) Large angle scattering at $s \gg M^2$, t/s fixed (Fig. 1b)

$$\frac{d\sigma}{dt}(AB \to CD) \sim \frac{1}{s^{n-2}} f(t/s) \tag{1.2}$$

where n = total number of constituent fields in A,B,C and D.

---

* Work supported by the Department of Energy under contract number EY-76-C-03-0515.
** Work supported in part by the National Science Foundation.

Talk presented at the Workshop on Current Topics in High Energy Physics, California Institute of Technology, Pasadena, CA., February 13-17, 1979.

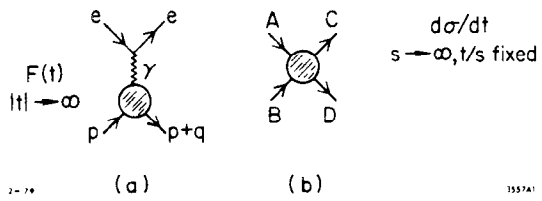

Fig. 1. Hadronic form factors and fixed angle exclusive scattering.

(c) Structure functions at $Q^2 >> M^2$, $\mathcal{M}^2 = \frac{1-x}{x} Q^2$ fixed:

$$F_{2H}(x,Q^2) \sim (1-x)^{2n_s-1}$$

where n_s = number of spectator fields in H.[3]

In each case the minimum number of fields dominates the asymptotic behavior. The rules follow simply from tree graphs in any renormalizable field theory if the four-momentum of each hadron is partitioned among its constituents.[1]

A comparison of the counting rule prediction $t^{n-1}F_H(t) \to$ const. for F_π, G_{M_p}, G_{M_n}, and F_D is shown in Figs. 2 and 3.

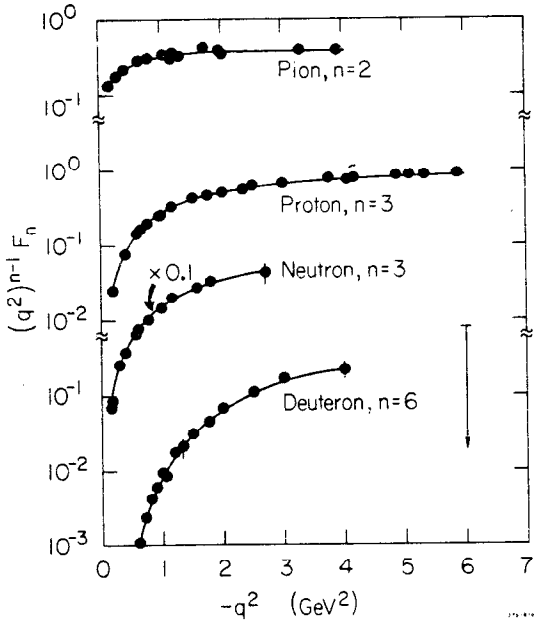

Fig. 2. Hadronic form factors multiplied by $(q^2)^{n-1}$. (From Ref. 5.)

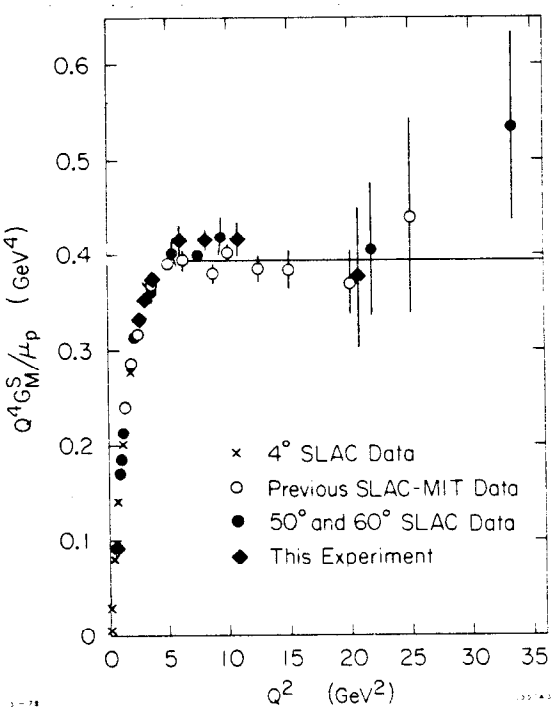

Fig. 3. The proton form factor G_M multiplied by $(Q^2)^2$. (From Ref. 6.)

In the case of the dueteron, the neutron and proton components evidentally each receive a momentum transfer ~q/2. It is thus con-

venient to define the "reduced" form factor[4,5]

$$f_D(Q^2) = \frac{F_D(Q^2)}{F_N^2(Q^2/4)} \tag{1.4}$$

The prediction $Q^2 f_D(Q^2) \to$ const. is compared with the data[7] in Fig. 4.

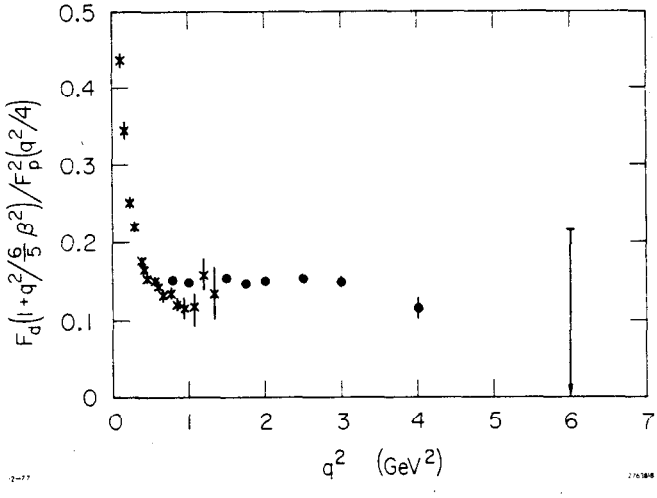

Fig. 4. The reduced deuteron form factor $f_D(q^2)$ multiplied by $(1-q^2/m_0^2)$ with $m_0^2 = 0.5$ GeV^2. (From Ref. 5.)

In the case of photoproduction at large angles, one predicts $d\sigma/dt(\gamma p \to \pi^+ n) \sim s^{-7} f(\theta_{cm})$, since the photon is an elementary field. The best fit to the 90° data[8] (Fig. 5a) is $s^{-7.3 \pm 0.4}$. The expectation that $d\sigma/dt(\gamma p \to \gamma p)/d\sigma/dt(\gamma p \to \pi^o p)$ increases with energy at fixed angle is borne out by the data[9] shown in Fig. 5b. Meson-baryon scattering data[10] at 90° is not inconsistent with the $s^{-8} f(\theta_{cm})$ prediction. In the case of proton-proton scattering, the prediction $d\sigma/dt \sim s^{-10} f(\theta_{cm})$ appears to be consistent with data over a large range of energies and angles (see Fig. 6). The overall best fit[11] is $s^{-9.7 \pm 0.5} f(\theta_{cm})$. A recent measurement[12] of $d\sigma/dt(pp \to pp)$ and $d\sigma/dt(np \to np)$ at $\theta_{cm} = 90°$ gives best fits $s^{-9.81 \pm 0.05}$ and $s^{-10.40 \pm 0.34}$, respectively. This apparent agreement with prediction is flawed however by the factor of two oscillations[13] in the data shown in Fig. 7. (We shall discuss in Section 7 a possible explanation for this effect as well as for the large spin correlations recently measured in pp-scattering at Argonne.[14])

The dimensional counting rules neatly summarize a wide range of large momentum transfer phenomena, and it is thus of considerable interest to see whether these rules are actual predictions of perturbative quantum chromodynamics. The general outlines of such a proof was given in Ref. 1, where it was noted that infrared effects which normally lead to Sudakov suppressions of the quark form factor are absent for hadron (color singlet) matrix elements. It was also conjectured that QCD would lead to logarithmic corrections to the scaling predictions, but the nature of these corrections was not understood.

In this talk we will present an outline of a new analysis of exclusive processes in QCD. (A detailed report will appear elsewhere.[15,16]) The main elements of this work involve a consistent Fock space decomposition of the hadronic wavefunction, plus evolution

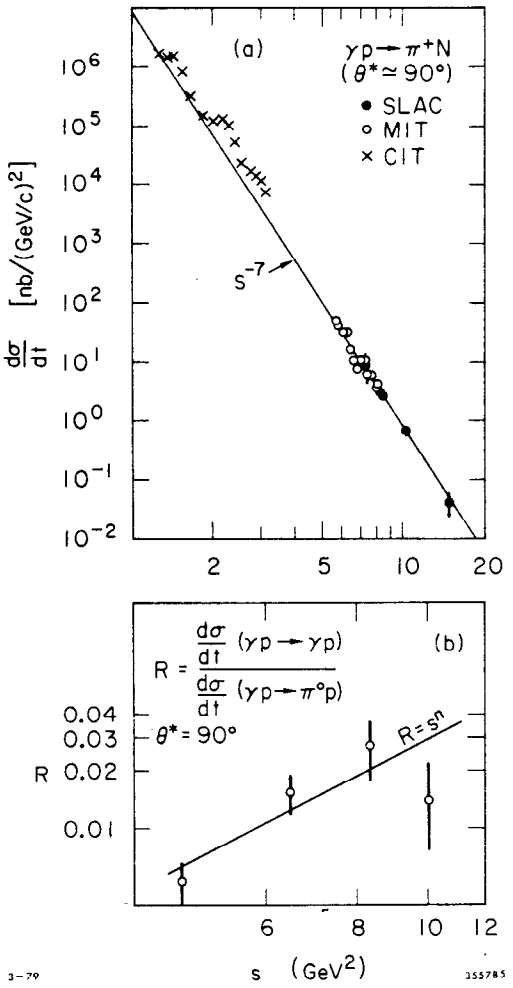

Fig. 5. (a) Pion photoproduction data at 90°. (From Ref. 8.) (b) Comparison of 90° Compton scattering and π^0 photoproduction. The best fit to the ratio is s^n with $n = 2.1 \pm 0.6$. (From Ref. 9.)

Fig. 6. Proton-proton elastic scattering at fixed θ_{cm}. (From Ref. 11.)

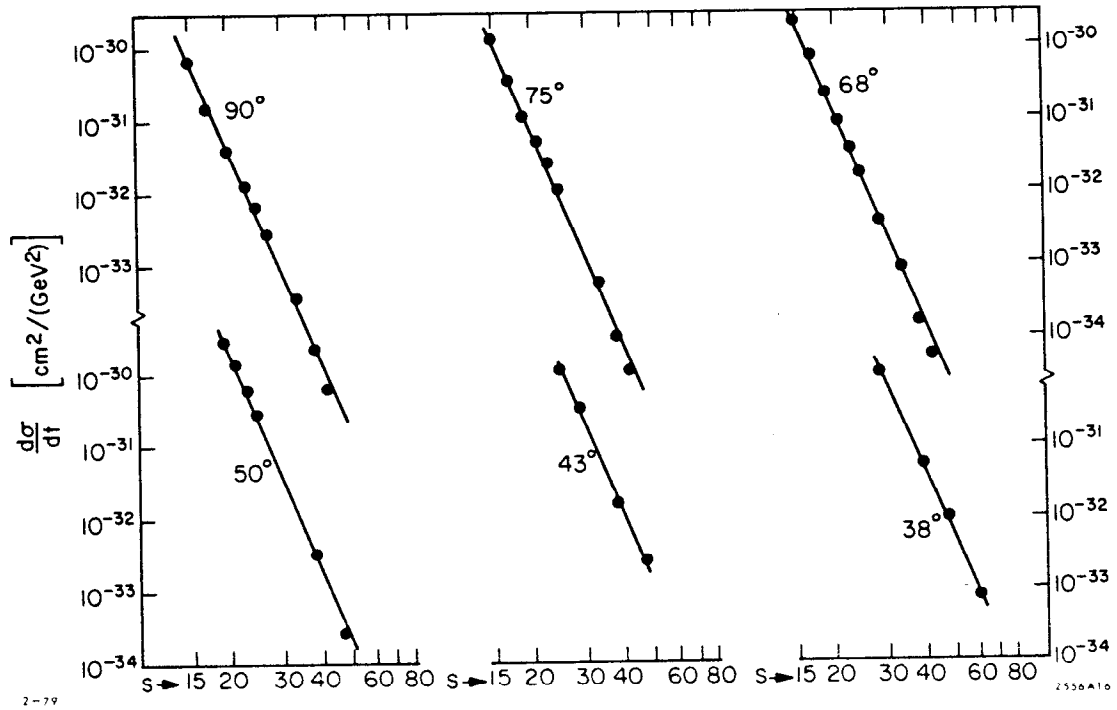

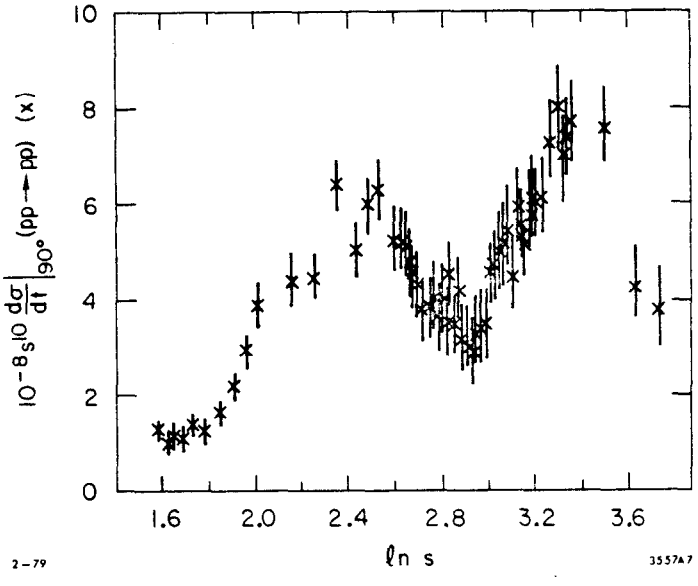

Fig. 7. Proton-proton scattering cross section at 90° multiplied by s^{10}. (From Ref. 13.)

equations for wave-functions which allow an exact evaluation of hadronic matrix elements in the asymptotic short distance limit. We are also collaborating with Y. Frishman and C. Sachrajda on an operator product analysis of these results.[16] Our analysis shows that the dimensional counting rules (1.1-3) are in fact predictions of quantum chromodynamics modulo calculable powers of the running coupling constant $\alpha_s(Q^2)$, i.e.: $\log^{-1} Q^2/\Lambda^2$. A central result is the prediction for the asymptotic form of the pion form factor:

$$F_\pi(Q^2) = 16\pi\, f_\pi^2 \frac{\alpha_s(Q^2/4)}{Q^2} \cdot \left[1 - c_2(\lambda^2)\left(\frac{\log Q^2/4\Lambda^2}{\log \lambda^2/\Lambda^2}\right)^{-\gamma_2} + c_4(\lambda^2)\left(\frac{\log Q^2/4\Lambda^2}{\log \lambda^2/\Lambda^2}\right)^{-\gamma_4} + \ldots\right]^2 \cdot \left[1 + O(\alpha_s(Q^2/4)) + O(m^2/Q^2)\right] \tag{1.5}$$

where $f_\pi = 94$ MeV is the pion decay constant normalized by the $\pi^+ \to \mu^+\nu$ decay amplitude, and we have used ($\beta = 11 - 2/3\, n_f$)

$$\exp \frac{\beta}{4\pi} \int_{-\lambda^2}^{-Q^2} \frac{d\ell^2}{\ell^2}\, \alpha_s(\ell^2) \cong \frac{\log Q^2/\Lambda^2}{\log \lambda^2/\Lambda^2} \tag{1.6}$$

The powers $\gamma_2 \cong 0.62$, $\gamma_4 \cong 0.90$, etc., are the usual non-singlet anomalous dimensions in QCD, which in this case appear as eigenvalues for the evolution equation for the $q\bar{q}$ meson Fock state.

We have recently learned that the prediction $F_\pi(Q^2) \to c f_\pi^2 \alpha_s(Q^2)/Q^2$ was in fact already derived by Farrar and Jackson[17] using the Feynman gauge ladder approximation to the Bethe-Salpeter equation for the pion in QCD. However, the Bethe-Salpeter kernel requires an

infinity of crossed ladder diagrams in covariant gauge even when working in the leading log approximation. This result also appears in a recent report by Efremov and Radyushkin[18] who assume the validity of a particular short distance operator product expansion of the hadronic form factor. The possibility of utilizing products of local fields as hadronic interpolating fields to derive the dimensional counting rules has also been discussed by Polyakov.[19] A conformal group analysis has been given by Menotti.[20]

The graphical analysis utilized here builds on earlier work by Appelquist and Poggio[21] for ϕ^3 in six dimensions. Other early work includes analyses of Yukawa theories by Goldberger, Guth and Soper[22] and QCD in 2 dimensions by Brower, Einhorn, Ellis, Weis[23] and others.

2. Exclusive Processes in QCD

A convenient framework for the analysis of hadronic matrix elements in QCD is time-ordered perturbation theory in the infinite momentum frame; i.e.: quantization on the light-cone. The meson Fock state can be represented as a column vector Ψ with an infinite number of components corresponding to $\langle q\bar{q}|\Psi\rangle$, $\langle q\bar{q}g|\Psi\rangle$, etc. The bound state equation[24]

$$\Psi = SK\Psi \qquad (2.1)$$

is thus an infinite set of coupled equations where the matrix K is the irreducible kernel (see Fig. 8a). The meson form factor receives contributions from each Fock state component as indicated in Fig. 8b. The two particle $q\bar{q}$ Fock state component of the pion corresponds to the usual Bethe-Salpeter amplitude evaluated at equal relative "time" $x^+ = x^0 + x^3$. As we shall see, this amplitude is normalized by the local decay amplitude $\pi^+ \to W^+ \to \mu^+\nu$. The existence of components corresponding to a finite number of constituents is only possible for a color singlet state.[25]

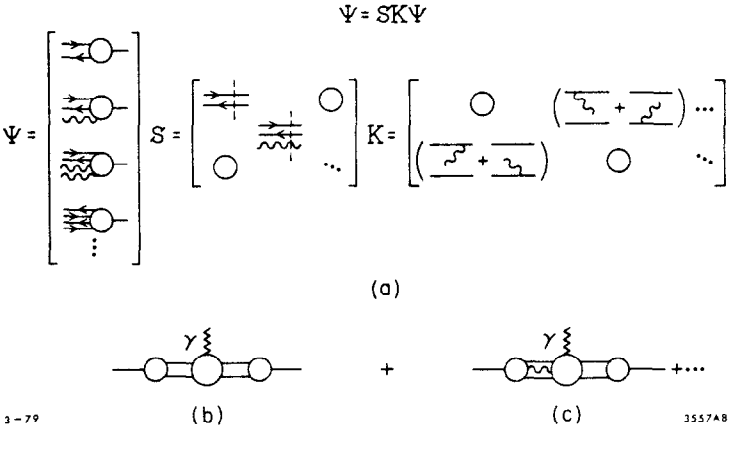

Fig. 8. (a) The meson bound state equation in time-ordered perturbation theory.
(b) The meson form factor in TOPTh.

The n-particle propagator in momentum space is

$$S^{-1}_{(n)} = M^2 - \sum_i^n \frac{\vec{k}^2_{\perp i} + m_i^2}{x_i} + i\varepsilon \qquad (2.2)$$

where $x_i = x_i^+ = \frac{(k_0 + k_3)_i}{(p_0 + p_3)}$ is the fractional momentum variable:

$$\sum_{i=1}^{n} x_i = 1$$

We can separate hard and soft components in the wave function by defining the propagator

$$S_\lambda = \begin{cases} 0 & \text{if} \quad \left| M^2 - \sum \frac{\vec{k}^2_\perp + m^2}{x} \right| > \lambda^2 \\ S \end{cases} \qquad (2.3)$$

Thus S_λ vanishes for virtual states far-off the energy shell; in particular $S_\lambda = 0$ if any constituent has large transverse momentum $k_\perp > \lambda$ relative to the direction of the bound state. We then can write

$$\begin{aligned} \Psi &= S_\lambda K \Psi + (S - S_\lambda) K \Psi \\ &= \Psi_\lambda + \Delta S K \Psi \\ &= \Psi_\lambda + \Delta S K \Psi_\lambda + \Delta S K \Delta S K \Psi_\lambda + \ldots \end{aligned} \qquad (2.4)$$

i.e.: the "hard" component of the wavefunction can be obtained by perturbation theory from the wavefunction derived in the soft regime (see Fig. 9). This expansion is convergent since only far off shell propagation occurs in intermediate states: $\Psi_\lambda = S_\lambda K \Psi$ contains all non-perturbative effects; $\Delta S = S - S_\lambda$ vanishes in the non-perturbative region. (Note that without the cutoff λ^2 the series in ΔS diverges because of bound state poles in the Green's functions.) An analogous technique for separating hard and soft regimes has been used in Ref. 26 to systematically treat high order radiative corrections to the positronium spectrum. The renormalization program can be

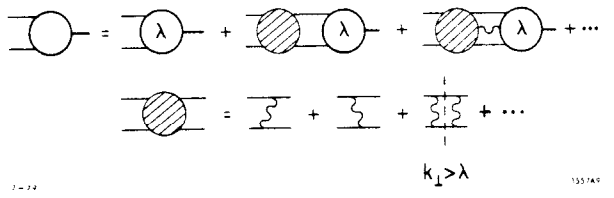

Fig. 9. The $q\bar{q}$ Fock state wavefunction of the meson using Eq. (2.4). The two particle reducible amplitudes in the kernel only contribute for $k_\perp > \lambda$.

implemented as discussed in Refs. 26 and 27.

The pion form factor can now be represented as a sum of matrix elements between Ψ_λ states (see Fig. 10). Notice that all connected diagrams (reducible and irreducible) contribute to the hard scattering amplitude. As we shall show, there are no singularities from the phase-space factors at $x_i \to 0$. By definition the transverse momenta in the amplitudes are regulated by λ. All nonperturbative effects in the form factor amplitude are contained in Ψ_λ.

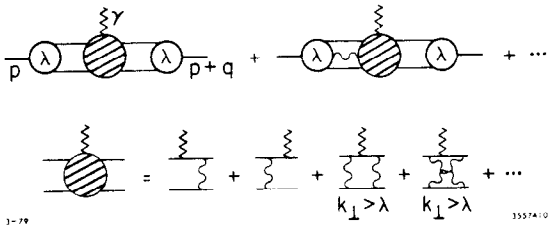

Fig. 10. The meson form factor in QCD using the S division. All Fock states contribute.

It is easy to check by dimensional analysis/power counting that Fock components which contain more than the minimum number of quarks in Ψ_λ give contributions to the form factor which are power law suppressed: the nominal power is (see Fig. 11)

$$F(Q^2) \sim \left(\frac{1}{Q^2}\right)^{n_q - 1} \tag{2.5}$$

An analogous statement also holds for extra gluons in the Fock state, but the interpretation depends on the gauge choice. First we note that diagrams where a gluon connects the initial and final-state soft constituents are suppressed by a power of Q^2 because the hadron is a singlet and true infrared divergences cancel. (In the case of colored states such contributions lead to the analogue of the Sudakov form factor.) Diagrams where a soft gluon from Ψ_λ interacts with a hard quark as in Fig. 11b are also suppressed by a power of q^2 unless the gluon has polarization ε_+. In fact, contributions from any number of such gluons can be resummed (via the Ward identity) into an effective two particle wavefunction. Alternatively, one can simply choose the light-cone gauge $\eta \cdot A = 0$ for which $\varepsilon_+ = 0$, and the anomalous contributions are suppressed by higher power of Q^2.

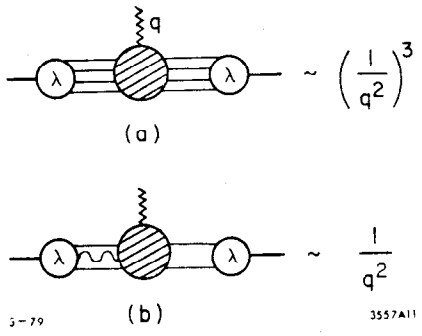

Fig. 11. Fock state contributions to the meson form factor. The $|qq\bar{q}\bar{q}\rangle$ amplitude (a) obeys Eq. (2.5). The $|q\bar{q}g\rangle$ amplitude (b) gives an anomalous contribution $O(Q^{-2})$ if $\varepsilon = \varepsilon_+$; in light cone gauge its contribution is $O(Q^{-4})$.

The calculation of the form factor have been performed in general covariant gauges as well as in the light-cone gauge, although for simplicity we will only present the light-cone gauge calculation here. All of the final results are gauge invariant. Note that Eq. (2.5) refers to Fock state constituents that are forced to change directions. Higher Fock state components in which the constituents annihilate before the exchange of the hard momentum Q only modify the form of the soft wavefunction Ψ_λ.

Thus contributions to the leading $1/Q^2$ power dependence of the meson form factor only arise (in the light-cone gauge) from the quark-antiquark Fock state component of the meson wavefunction (see Fig. 12). It is convenient to choose a Lorentz frame where q_μ is transverse to the direction of the incident meson ($-q^2 = Q^2 = 4\vec{q}_\perp^{\,2}$). It is then straightforward to identify the leading logarithmic corrections to the $1/Q^2$ power law in each order of perturbation theory. In fact, by using the light-cone gauge only the ladder diagrams are required. The neglected terms will be of relative order $\alpha_s(Q^2)$ and m^2/Q^2.

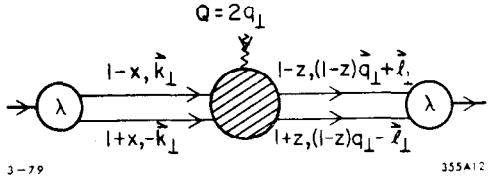

Fig. 12. Two-particle Fock state contribution to the meson form factor; the kinematics are chosen so that $x, z, \vec{k}_\perp$ and $\vec{\ell}_\perp$ vanish in the zero binding limit. Here $Q^2 = (2\vec{q}_\perp^{\,2})$.

To this order, the pion form factor in QCD takes the form (see Fig. 13) ($q^2 = -Q^2$)

$$F_\pi(Q^2) = \int_{-1}^{1} dx \int_{-1}^{1} dz\ \phi^+(z,Q^2/4)\ T_B(z,x,Q^2)\ \phi(x,Q^2/4) \qquad (2.6)$$

where ($C_F = 4/3$)

$$T_B = \frac{16\pi\alpha_s(Q^2/4)C_F}{Q^2}\ \frac{1}{(1+x)}\ \frac{1}{(1+z)} \qquad (2.7)$$

is the result expected from the simplest impulse approximation.

As we shall see, the wavefunction $\phi(x,Q^2)$ in Eq. (2.6), satisfies an evolution equation in QCD, and leads to non-trivial logarithmic modification

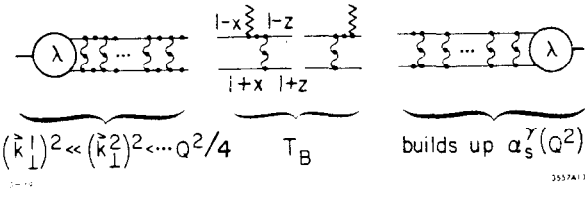

Fig. 13. Leading logarithm contributions to the meson form factor. The dominant momentum flow is through T_B. The ladder and self-energy insertions yield the evolution Eq. (2.14) and the anomalous dimensions in Eq. (2.15).

of dimensional counting. To leading order in $\alpha_s(Q^2)$, it is sufficient to compute the two-body wavefunction integrated over transverse momentum $\vec{k}_\perp^2 < Q^2$

$$\tilde{\phi}(x,Q^2) = \int_0^{Q^2} \frac{d\vec{k}_\perp^2}{16\pi^2} \psi(x, \vec{k}_\perp^2) \tag{2.8}$$

since the dominant momentum flow occurs through T_B. The leading contribution to order $\alpha_s(Q^2)$ can now be computed simply from the ladder graph structure with strong ordering of the loop momentum and the inclusion of all vertex and self-energy insertions as indicated in Fig. 13.

The wavefunction ϕ appearing in Eq. (2.6) is given by

$$\phi(x,Q^2) = \tilde{\phi}(x,Q^2) \left[\frac{\log Q^2/\Lambda^2}{\log \lambda^2/\Lambda^2} \right]^{-C_F/\beta} \tag{2.9}$$

where the last factor with $C_F = 4/3$ and $\beta = 11-2/3\ n_f$ is due to vertex and fermion self-energy corrections in T_B. By the Ward identity, such factors are process independent.

Because of the strong ordering of the $\vec{k}_\perp^2$ integrations, the integrated wavefunction obeys the inhomogeneous equation,

$$\tilde{\phi}(x,Q^2) = \tilde{\phi}(x,\lambda^2) + \int_{\lambda^2}^{Q^2} \frac{d\vec{k}_\perp^2}{\vec{k}_\perp^2} \frac{C_F}{4\pi} \alpha_s(\vec{k}_\perp^2) \int_{-1}^{1} dy\, V(x,y)\, \tilde{\phi}(y,\vec{k}_\perp^2) \tag{2.10}$$

where the kernel V is

$$V(x,y) = \frac{1-x}{1-y}\left(1 + \frac{2}{(x-y)_+}\right)\theta(x > y) + \frac{1+x}{1+y}\left(1 - \frac{2}{(x-y)_+}\right)\theta(y > x) \tag{2.11}$$

(This is the kernel for the quark and antiquark with opposite helicities, as required for pseudoscalar and $\lambda = 0$ vector meson states. In the case of parallel helicities, only the $2/(x-y)_+$ terms contribute.) The distributions in V are defined for integrals over x as

$$\frac{1-x}{1-y}\frac{2}{(x-y)_+}\theta(x>y) = \frac{1-x}{1-y}\frac{2}{x-y}\theta(x-y) - \delta(x-y)\int_y^1 dz\ \frac{1-z}{1-y}\frac{2}{z-y} \tag{2.12}$$

Thus there are no actual singularities as $x = y$. This infrared cancellation is due to the self-energy corrections to the q and $\bar{q}$ legs in Fig. 13; it would not occur if the constituents formed a non-singlet.

If we define

$$\xi = \frac{\beta}{4\pi} \int_{\lambda^2}^{Q^2} \frac{d\vec{k}_\perp^2}{\vec{k}_\perp^2} \alpha_s(\vec{k}_\perp^2) \cong \log \frac{\alpha_s(\lambda^2)}{\alpha_s(Q^2)} , \qquad (2.13)$$

then ϕ satisfies an evolution equation:

$$\frac{\partial}{\partial \xi} \phi(x,\xi) = \frac{C_F}{\beta} \int_{-1}^{1} dy\, V(x,y)\, \phi(y,\xi) - \frac{C_F}{\beta} \phi(x,\xi) \qquad (2.14)$$

These results are analogous to the evolution equations[28] derived for the ξ-dependence of non-singlet structure functions. In each case, infrared divergences cancel and procedures are available to evaluate the higher order corrections in $\alpha_s(Q^2)$. An essential difference is that the short-distance operator T_B is an integral over x rather than a delta-function.

The physics of the evolution equation for $\phi(x,\xi)$ is contained in the eigenvalues and eigenfunctions of $V(x,y)$. The general solution is

$$\phi(x,\xi) = (1-x^2) \cdot \sum_{n=0,2,4} a_n\, C_n^{3/2}(x) \left(\frac{\log Q^2/\Lambda^2}{\log \lambda^2/\Lambda^2} \right)^{-\gamma_n} \qquad (2.15)$$

Only terms even under $x \to -x$ occur in the pion wave function when SU(2) symmetry is assumed.

Here $C_n^{3/2}(x)$ is a Gegenbauer polynomial, e.g.,

$$C_n^{3/2}(x) = \begin{cases} 1 & n = 0 \\ -3/2(1 - 5x^2) & n = 2 \\ 15/8(1 - 14x^2 + 21x^4) & n = 4 \end{cases} \qquad (2.16)$$

The weights a_n are determined from the initial wavefunction

$$a_n = \frac{2n+3}{2(2+n)(1+n)} \int_{-1}^{1} dx\, \phi(x,\lambda^2)\, C_n^{3/2} \qquad (2.17)$$

and the γ_n are the standard non-singlet anomalous dimensions (taking $\beta = 9$)

$$\gamma_n = \frac{C_F}{\beta}\left\{1 + 4\sum_{2}^{n+1}\frac{1}{k} - \frac{2}{(n+1)(n+2)}\right\} \cong \begin{cases} 0 & n=0 \\ .62 & n=2 \\ .90 & n=4 \end{cases} \quad (2.18)$$

(The only assumption needed here is that the initial wavefunction $\phi(x,\lambda^2)$ falls as $(1-x^2)^\epsilon$ with $\epsilon > 0$ at $x = \pm 1$, which is in fact required by self-adjointness of the kinetic energy for the bound state wavefunction. This boundary condition can in fact be regarded as the condition of compositeness of the meson; if there were an elementary field with the quantum numbers of the meson then $\phi(x,\lambda^2)$ would be constant as $x^2 \to 1$ due to the possible $\bar{\psi}\gamma_5\psi$ coupling. Of course in this case $F_\pi(Q^2) \to$ const. In fact this type of analysis is required in the case of the photon structure function and transtion form factors in QCD.)

In the asymptotic limit $Q^2 \to \infty$, we have from Eq. (2.15)

$$\phi(x,Q^2) \to \frac{3}{4} k_\pi (1-x^2) \quad (2.19)$$

where

$$k_\pi = \lim_{Q^2\to\infty}\left[\frac{\log Q^2/\Lambda^2}{\log \lambda^2/\Lambda^2}\right]^{-C_F/\beta} \int_{-1}^{1} dx \int^{Q^2} \frac{d\vec{k}_\perp^2}{16\pi^2}\,\psi(x,\vec{k}_\perp) \quad (2.20)$$

Notice that the singularity of T_B at $x=-1$ or $z=-1$ is damped by the wavefunction. This should be contrasted with the situation for theories such as QCD in two-dimensions or ϕ^3 field theory where $T_B \sim (1+x)^{-2}(1+z)^{-2}$ and power-law modifications to the form factor can and do occur from this infrared, long distance region.[23]

We thus see from Eqs. (2.6) and (2.7) that in the asymptotic limit

$$F_\pi(Q^2) \underset{Q^2\to\infty}{\to} \frac{16\pi\alpha_s(Q^2/4)\,C_F}{Q^2}\left(\frac{3}{2}k_\pi\right)^2 . \quad (2.21)$$

In fact, we can determine the normalization from the weak decay amplitude for $\pi \to \mu\nu$:

$$f_\pi = \sqrt{n_c}\,k_\pi \sim 94 \text{ MeV} \quad (2.22)$$

i.e.:

$$F_\pi(Q^2) \underset{Q^2\to\infty}{\to} \frac{36\pi\alpha_s(Q^2/4)}{Q^2}\,\frac{f_\pi^2 C_F}{n_c} \qquad (2.23)$$

where n_c is the number of colors.

Although Eq. (2.23) gives the asymptotic form factor, the anomalous dimension terms result in sizeable corrections until very large momentum transfer, and in fact tend to compensate for the fall-off due to $\alpha_s(Q^2)$ over a wide range of Q^2. If we assume that $\phi(x,\lambda^2)$ is peaked at $x\sim 0$ (equal momentum partition) as is characteristic of non-relativistic bound states, then the evolution equation causes $\phi(x,Q^2)$ to broaden asymptotically out to the $(1-x^2)$ envelope where T_B is maximum (see Fig. 14). Thus one obtains Eq. (1.5) where $c_2 = -a_2/a_0$ and $c_4 = a_4/a_0$ are positive, and are computed from Gegenbauer moments of the soft wavefunction. The form factor is of course independent of the choice of λ^2. Figure 15 shows the prediction for $Q^2F_\pi(Q^2)$ assuming that $\phi(x,\lambda^2)$ is either strongly peaked at $x=0$ or has a smooth $(1-x^2)$ dependence.

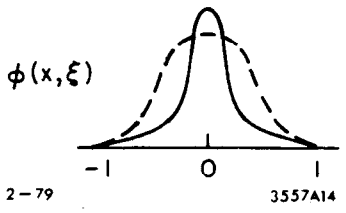

Fig. 14. Schematic representation of wavefunction evolution. As $Q^2\to\infty$, $\phi(x,Q^2)\to(1-x^2)$.

It is of course significant that the same anomalous dimensions enter in the pion form factor and the moments of the non-singlet structure function. This can be attributed to the fact that the leading local operators which couple to the pion wavefunction at short distances $x_\mu \to 0$ are the usual twist 2 $\bar\psi\gamma_\mu\gamma_5(D_\mu)^n\psi$ operators for $O_F^{(n)}$. The absence of an anomaly in the axial vector operator implies that the asymptotic form factor is of the form of Eq. (2.23).

In the case of vector mesons with total helicity ± 1, T_B vanishes as a power

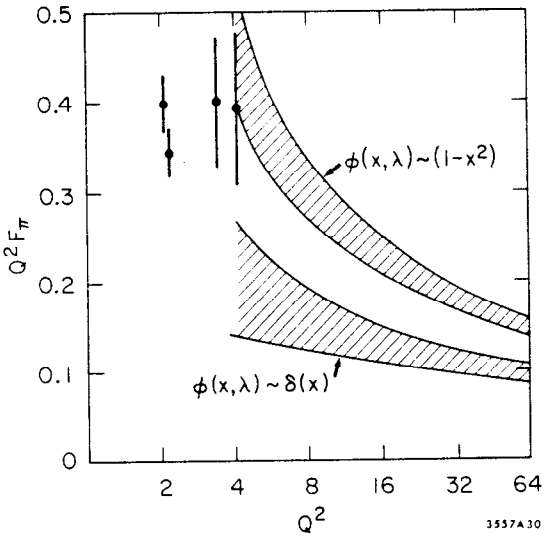

Fig. 15. QCD prediction for the meson form factor for two extreme cases: (a) $\phi(x,\lambda^2)\sim\delta(x)$, or (b) $\phi(x,\lambda^2)\sim(1-x^2)$. In the latter case the wavefunction is unchanged under evolution. The asymptotic predictions are absolutely normalized using Eq. (2.23). The bands correspond to $\pm\alpha_s/\pi$ with $\Lambda^2 = 0.25$ GeV^2.

of Q^2 faster than (2.7), and the potential only contains the $1/(x-y)_+$ term. Thus we obtain asymptotic forms

$$F_\rho(Q^2) \propto \begin{cases} F_\pi(Q^2) & \lambda_\rho = 0 \\ \dfrac{m^2(Q^2)}{Q^2}\ \dfrac{\alpha_s(Q^2)}{Q^2}\ [\alpha_s(Q^2)]^{2C_F/\beta} & \lambda_\rho = \pm 1 \end{cases} \qquad (2.24)$$

where $m(Q^2)$ is the "running mass" in QCD. Another contribution of order $1/Q^4$ can also evidently be obtained from the $n = 3|q\bar{q}g\rangle$ Fock state component of the vector meson wavefunction.

The transition form factor of the photon, e.g., $\gamma(Q^2) + \gamma(k^2 \sim 0) \to \pi^o$ can be analyzed in a similar fashion. We find

$$F_{\pi\gamma}(Q^2) = \frac{\left(e_u^2 + e_d^2\right) 2\sqrt{n_c}}{Q^2} \int_{-1}^{1} dx\ \frac{\phi(x,Q^2)}{1+x} \quad . \qquad (2.25)$$

(The $\gamma^*\gamma\pi^o$ vertex is defined as $ie^2\ F_{\pi\gamma}(Q^2)\ \epsilon_{\mu\nu\rho\sigma}\ p_\pi^\nu\ q^\rho\ \varepsilon^\sigma$.) This can be absolutely normalized in terms of the pion form factor

$$F_{\pi\gamma}(Q^2) = \frac{\left(e_u^2 + e_d^2\right) 2\sqrt{n_c}}{Q^2} \left[\frac{Q^2 F_\pi(4Q^2)}{4\pi\, C_F\, \alpha_s(Q^2)}\right]^{1/2} \quad . \qquad (2.26)$$

The corrections are of order $O[\alpha_s(Q^2)]$.

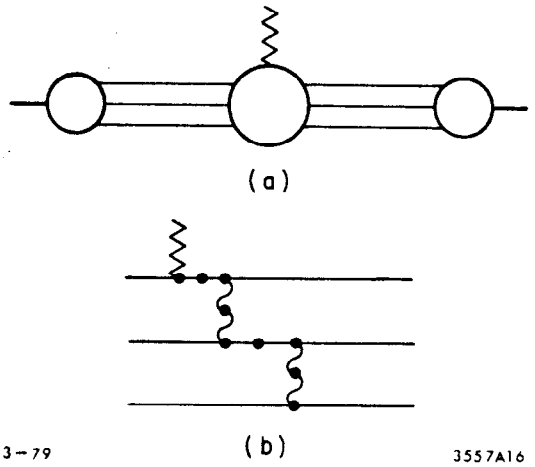

Fig. 16. Schematic representation of the nucleon form factor for the three quark Fock state.

The form factor of nucleons may be analyzed in a similar manner. The leading power law terms arise from the minimal 3 quark Fock component and gives $T_B \sim [\alpha_s(Q^2)/Q^2]^2$ (see Fig. 16). A three body kernel and evolution equation can then be obtained in parallel with the meson case. The asymptotic result is

$$F_1(Q^2) \sim \frac{\alpha_s^2(Q^2)}{(Q^2)^2}\left(\sum_j a_j(\log Q^2/\Lambda^2)^{-\gamma_j(N)}\right)^2 \qquad (2.27)$$

$$F_2(Q^2) \sim \frac{M\cdot m(Q^2)}{Q^2} F_1(Q^2) \qquad (2.28)$$

The calculation of the nucleon anomalous dimensions $\gamma_j(N)$ is in progress.[15] These results agree with the dimensional counting predictions and verify that the empirical $G_M \sim G_E \sim 1/Q^4$ scaling laws are consistent with quantum chromodynamics, modulo over-all $\log Q^2$ corrections.

3. The Inclusive-Exclusive Connection

The above predictions for the form of the asymptotic form factor may seem somewhat paradoxical since QCD asymptotic freedom corrections to Bjorken scaling of hadronic structure functions appear to be relatively much stronger. In particular, as shown in Ref. 29, QCD predicts structure functions at large x of the form

$$F_2(x,Q^2) \sim (1-x)^{V+\tilde{\xi}(Q^2,k^2)} P(\tilde{\xi}) \qquad (3.1)$$

where $(1-x)^V$ is the effective power-behavior at $Q^2 \sim O(k^2)$, and

$$\tilde{\xi}(Q^2,k^2) = \frac{C_F}{\pi}\int_{k^2}^{Q^2}\frac{d\ell^2}{\ell^2}\alpha_s(\ell^2) \sim O(\log\log Q^2) \; . \qquad (3.2)$$

and $P(\tilde{\xi})$ is a normalization factor.[29] If one uses this form for fixed $\mathcal{M}^2 = \frac{1-x}{x} Q^2$; then one obtains transition form factors

$$F^2(Q^2) \sim \left(\frac{\mathcal{M}^2}{Q^2}\right)^{V+1+\tilde{\xi}(Q^2,k^2)} P(\tilde{\xi}) \qquad (3.3)$$

which fall faster than any power![30]

In fact, this "derivation" is incorrect in the fixed $\mathcal{M}^2$, high Q^2 domain because it ignores the fact that the struck hadronic constituent is far off-shell. In general the constituent mass that sets the lower limit in the $\tilde{\xi}$ integration is given by

$$k^2 = z\left[M_H^2 - \frac{k_\perp^2 + \tilde{m}^2}{1-z} - \frac{k_\perp^2}{z}\right] \qquad (3.4)$$

where $\tilde{m}^2$ is the square of the invariant mass of the remaining spectators and $\vec{k}_\perp$ and z are the struck constituent's light-cone coordinates in the hadronic wavefunction. Since $z > x$, and x is near 1,

$$-k^2 \sim \frac{k_\perp^2 + \tilde{m}^2}{1-x} \sim \frac{k_\perp^2 + \tilde{m}^2}{\mathcal{M}^2} Q^2 \tag{3.5}$$

i.e.: $k^2 \sim O(Q^2)$ at fixed $\mathcal{M}^2$. Thus

$$\tilde{\xi} = \frac{4C_F}{11-2/3\, n_f} \log \frac{\alpha_s(k^2)}{\alpha_s(Q^2)} \tag{3.6}$$

$$\Rightarrow \frac{C_F}{\pi} \alpha_s(Q^2) \log\left(\frac{\mathcal{M}^2}{\vec{k}_\perp^2 + \tilde{m}^2}\right) \text{ at fixed } \mathcal{M}^2,\ Q^2 \to \infty.$$

i.e.: $\tilde{\xi}$ actually vanishes as $1/\log Q^2$ in the fixed $\mathcal{M}^2$ domain.

The behavior of structure functions in the large x region can be computed in leading order in α_s from the infinite set of diagrams indicated in Fig. 17. The infinite set of horizontal gluon ladder graphs above the quark leg labeled k^2 in the figure builds up the standard QCD corrections to Bjorken scaling and q^2 dependence of the structure function moments. The main power law dependence at $x \sim 1$ is given by the minimal number of (vertical) gluon exchanges required to stop the hadronic spectators. For the case of the nucleon the leading Fock state component is the $|qqq\rangle$ state, and two gluon exchanges with off-shell masses of order $k_x^2 \sim O((\vec{k}_\perp^2 + \tilde{m}^2)/(1-x))$ are required. These minimal hard gluon exchange diagrams give the analogue of T_B in the form factor calculation.

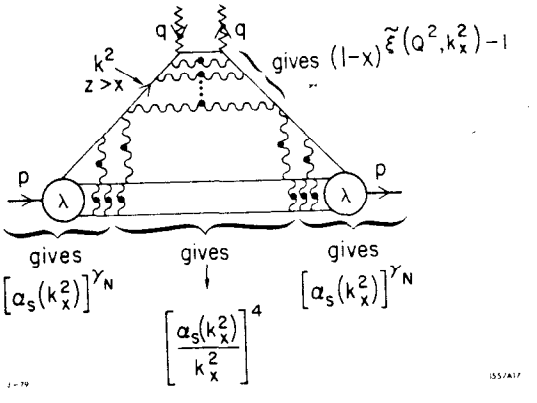

Fig. 17. Analysis of deep inelastic scattering (virtual Compton amplitude) to leading logarithmic order in perturbation theory. See Eq. (3.7).

In addition, the remaining infinite set of vertical gluon exchange diagrams (ordered, as usual, in momenta) leads to the evolution of the hadronic wavefunction from the soft region λ^2 to the off-shell value k_x^2. As in the form factor calculation, this leads to a series of anomalous logarithms $[\alpha_s(k_x^2)]^{\gamma_j(N)}$ determined by the eigenvalues of the kernel for the Fock state. Combining factors, the leading behavior is given by

$$F_{2N}(x,Q^2) \sim C(\tilde{\xi})(1-x)^{3+\tilde{\xi}(Q^2,k_x^2)}\ \alpha_s^4(k_x^2) \cdot \left[\sum_j a_j (\log k_x^2/\Lambda^2)^{-\gamma_j^{(N)}}\right]^2 \qquad (3.7)$$

where the $\gamma_j^{(N)}$ are the leading anomalous dimension for the 3-quark nucleon wavefunction. Correction terms of higher power in (1-x) and $\alpha_s(Q^2)$ or $\alpha_s(k_x^2)$ are neglected. Notice that at fixed $\mathcal{M}^2$, $\tilde{\xi} \to 0$ and we obtain a perfect exclusive-inclusive connection with the corresponding form factor claculation Eq. (2.7), in agreement with the Drell-Yan-West relation.

Equation (3.7) is consistent with the standard evolution equations for QCD structure functions and moments and other results derived from the operator product expansion.[31,32] In the large x domain, however, the "initial" or "starting" structure function is no longer unknown but is directly determined from QCD perturbation theory and the wavefunction evolution equations at short distances. In a sense the most critical prediction from QCD is the nominal power law $(1-x)^3$ since the integer 3 reflects the existence of a 3 quark Fock state as well as nearly scale-invariant QCD quark-quark interactions within the nucleon. The logarithmic dependence from $\tilde{\xi}(Q^2,k_x^2)$ and $\alpha_s(k_x^2)$ in Eq. (3.7) yield the radiative corrections to the main dynamical dependence of the structure function. The predicted form for the structure function may prove useful for fits to data, at least for $x > 0.5$.

In practice, the expected values of $\tilde{\xi}$ are not large (e.g., for $Q^2 = 100$ GeV^2, $k_x^2 = 1$ GeV^2, and $\Lambda^2 = 1/3$ GeV^2, $\tilde{\xi} \cong 1$) so the observed (1-x) power should be typically less than one unit larger than the valence power. The direct measurement of the leading power behavior of the valence state structure function requires the determination of the structure function at fixed $\mathcal{M}^2$ over a large range of Q^2.

It should be noted that the form of Eq. (3.7) complicates the empirical analysis of moments at large N. In general

$$\mathcal{M}_N(Q^2) = \int_0^{1-\Delta M^2/Q^2} dx\, x^{N-1}\, F_2(x,Q^2) = \left[\frac{\alpha_s(Q^2)}{\alpha_s(\bar{k}_N^2)}\right]^{\gamma_N} \qquad (3.8)$$

(The elastic contribution gives a power-law correction to Bjorken scaling.) At large N, only large x is important and

$$\bar{k}_N^2 \sim O\left\langle \frac{\tilde{m}^2 + \vec{k}_\perp^2}{1-x} \right\rangle \sim O\left(\frac{\tilde{m}^2 + \vec{k}_\perp^2}{\Delta M^2} \right) Q^2 \qquad (3.9)$$

Thus $\mathcal{M}_N(Q^2)$ tends to scale in the large N limit, again because of the strong off-shell behavior of the struck constituent. The standard QCD prediction $\mathcal{M}_N(Q^2) \sim [\alpha_s(Q^2)]^\gamma N$ only holds for Q^2 sufficiently large such that $\Delta M^2/Q^2 \ll N^{-1}$.

4. Quark Sea Phenomenology

The decomposition of the nucleon wavefunction in terms of its Fock state components $|qqq\rangle$, $|qqqg\rangle$, $|qqqq\bar{q}\rangle$, etc. leads to a new perspective on the origin of the phenomenological sea quark distributions (see Fig. 18). The "intrinsic" sea from the $|qqqq\bar{q}\rangle$ component has a nominal power dependence at large x

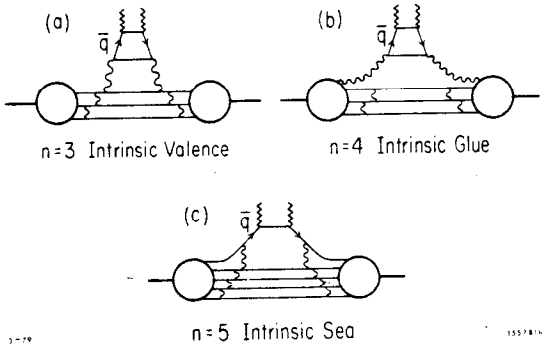

Fig. 18. Intrinsic versus evolved contributions to the nucleon sea quark distribution:
(a) quark sea evolved from the $|qqq\rangle$ valence state;
(b) quark sea evolved from the intrinsic gluon distribution;
(c) intrinsic sea contribution.

$$F_2^{\bar{q}} \propto (1-x)^{7+\tilde{\xi}} \qquad (4.1)$$

since there are 4 spectators.[34] The sea quarks which evolve in Q^2 due to lowest order pair production from the intrinsic gluons in the $|qqqg\rangle$ components lead to a contribution of the form

$$F_2^{\bar{q}} \propto \tilde{\xi}(1-x)^{5+\tilde{\xi}} \qquad (4.2)$$

Similarly, the sea quarks evolved from the $|qqq\rangle$ valence component via gluon bremsstrahlung and subsequent pair production lead to a contribution

$$F_2^{\bar{q}} \propto \tilde{\xi}^2(1-x)^{5+\tilde{\xi}} \qquad (4.3)$$

In general, the measured distribution should be a Q^2-dependent sum of such contributions.

At fixed $\mathcal{M}^2$, $\tilde{\xi} = \tilde{\xi}(Q^2, k_x^2) \to 0$, and thus despite the extra power of (1-x) the intrinsic sea components could be particularly important in this domain. Further, as has been shown in Ref. 33, there are strong cancellations between various contributions to the gluon distribution in hadrons at low momentum due to the singlet nature of the source.

The intrinsic sea quark component may in fact be numerically dominant until very large Q^2. In that case we expect the nominal power of $F_2^{\bar{q}}(x,Q^2)$ at large x to decrease from $(1-x)^7$ to $(1-x)^5$ as the evolved component become relatively stronger.

5. Pion Structure Functions

The structure functions of mesons can also be analyzed at large Q^2 and small (1-x) in a manner similar to the analysis of nucleon structure functions. In this case, as first noted by Ezawa,[35] there is a kinematic suppression of the transverse cross section $\sigma_T(Q^2)$ by a power of (1-x) which can be attributed to the mismatch between the spin of the quark and spin of the meson. In our analysis this shows up in the corresponding suppression of the tree diagrams for T_B at x near 1. Since the meson wavefunction has a leading zero anomalous dimension,

$$F_2^\pi(x,Q^2) \sim (1-x)^{2+\tilde{\xi}} \log^{-2}\left(\frac{1}{1-x}\right)$$

$$Q^2 \to \infty \quad , \quad (1-x) \text{ small} \tag{5.1}$$

In addition, it is important to note that the longitudinal structure function has an anomalous (non-scaling) component which is nearly flat at large x:[36,37]

$$F_L^\pi(x,Q^2) \sim \frac{(1-x)^{0+\tilde{\xi}}}{Q^2} \log^{-2}\left(\frac{1}{1-x}\right) \tag{5.2}$$

where $\tilde{\xi} \sim \tilde{\xi}(Q^2,k_x^2)$. If we analyze this in the fixed $\mathcal{M}^2$ domain, then $\tilde{\xi} \to 0$ and

$$F_2^\pi(x,Q^2) \to F_L^\pi(x,Q^2) \sim (1-x) \log^{-2}\left(\frac{1}{1-x}\right)$$

$$Q^2 \to \infty \quad , \quad \mathcal{M}^2 \text{ fixed} \tag{5.3}$$

Thus, as in the nucleon case, there is a perfect exclusive/inclusive connection. The dominance of the longitudinal structure function in the fixed $\mathcal{M}^2$ limit for mesons is an essential prediction of perturbative QCD. It can be tested directly[36] in the $e^+e^- \to \pi X$ angular distribution near the kinematic boundary ($x \to 1$). Perhaps the most dramatic consequence is in the Drell-Yan process $\pi p \to \mu^+\mu^- X$ (Fig. 19). In this case one predicts[38] that for fixed Q^2 pairs, the angular distribution of the μ^+ (in the pair rest frame) will change from the conventional $(1+\cos^2\theta_+)$ distribution to $\sin^2\theta_+$ for pairs produced at large longitudinal momentum, $x_L(\mu^+\mu^-) \to 1$. This is due to the

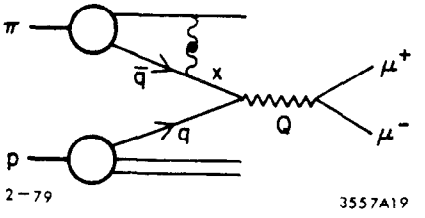

Fig. 19. Representative contribution to Drell-Yan $\pi p \to \mu^+\mu^- X$ cross section. The gluon exchange in the pion wavefunction is responsible for the power law fall off at $x \to 1$ [Eq. (5.1-3)] and the power law tail at large $k_\perp^2$ [Eq. (8.1)].

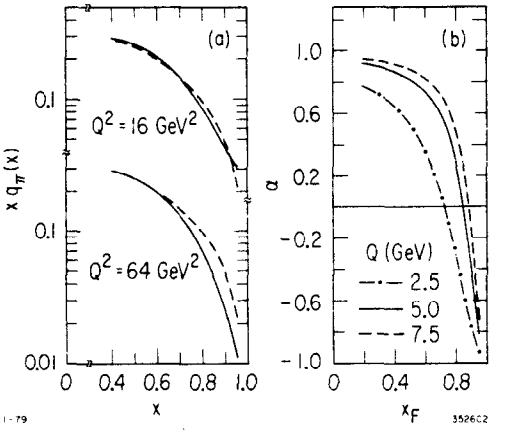

Fig. 20. (a) The pion structure function at large x. The solid line is the prediction $F_2^\pi \sim (1-x)^2 + C/Q^2$. (b) Prediction for the μ^+ angular distribution $1 + \alpha\cos^2\theta_+$ where θ_+ is measured relative to the incident pion in the $\mu^+\mu^-$ rest frame. (From Ref. 38.)

dominance of the meson's longitudinal structure function at large x and fixed Q^2 (see Fig. 20b). Figure 20a also shows that the predicted form of the structure function $F_2^\pi(x,Q^2) \sim (1-x)^2 + C/Q^2$ is not inconsistent with recent fits to the data. The dashed line is the experimental form $(1-x)^{1.01}$ given in Ref. 39.

6. Fixed Angle Scattering

The techniques which we have discussed for obtaining asymptotic results for form factors can be extended to the computations of any exclusive process involving large momentum transfer between color singlets. Here we shall focus on fixed angle hadronic scattering $d\sigma/dt(A+B \to C+D)$ as $s \to \infty$ at fixed t/s or θ_{cm}. In general, each hadron is represented by its Fock state decomposition; the leading power law dependence as $s \to \infty$ is obtained from the Fock state with the minimum number of interacting components. The analysis of fixed angle scattering is complicated by pinch singularities, so we must consider two different scattering mechanisms.

A. Hard Subprocesses

In this case the momentum transfer between constituents occurs through a single hard scattering amplitude T_B with all internal legs off-shell and proportional to $p_T^2 = tu/s$. The fixed angle amplitude is then to leading order in $\alpha_s(p_T^2)$ (see Fig. 21),

$$\mathcal{M}_{AB\to CD} = \int \prod_i dx_i\ \phi_C^+(x_c,p_T^2)\ \phi_D^+(x_d,p_T^2)\ T_B(x_i,p_T^2)\ \phi_A(x_a,p_T^2)\ \phi_B(x_b,p_T^2) \qquad (6.1)$$

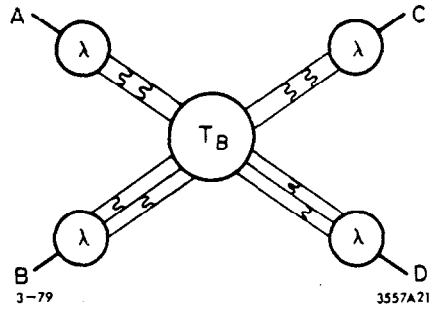

Fig. 21. Fixed angle scattering in QCD for hard subprocesses (see Eq. (6.1)).

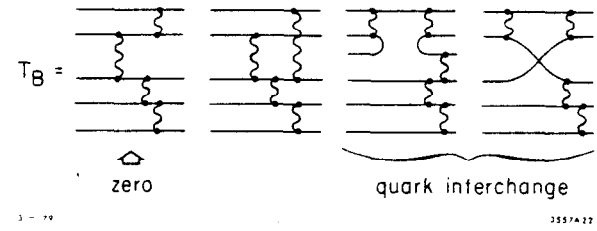

Fig. 22. Examples of hard scattering processes for πp elastic scattering.

The amplitude T_B yields the power-law fall-off $p_T^{-(n-4)}$ where n is the total number of constituents, in agreement with the dimensional counting rule.[1,2] Examples of the leading contributions to lowest order in $\alpha_s(p_T^2)$ for meson-baryon scattering are shown in Fig. 22. Single gluon exchange between color singlet hadrons is of course zero. The constituent interchange graphs,[40] Fig. 22c,d, are among the dominant contributions and lead to large flavor-exchanging amplitudes.

As in the form factor calculation, the evolution of the wavefunctions $\phi(x,\lambda^2)$ to $\phi(x,p_T^2)$ yields a series of terms with anomalous powers of $\alpha_s(p_T^2)$. The asymptotic cross section at $p_T^2 \to \infty$ has the form

$$\frac{d\sigma}{dt}(A+B \to C+D) \Longrightarrow \frac{[\alpha_s(p_T^2)]^{n-2+\sum_I \gamma_I}}{[p_T^2]^{n-2}} f(\theta_{cm}) \qquad (6.2)$$

$$= \frac{\alpha_s^2(p_T^2)}{p_T^2} F_A(p_T^2)\, F_B(p_T^2)\, F_C(p_T^2)\, F_D(p_T^2)\, f(\theta_{cm}) \qquad (6.3)$$

where γ_I is the leading anomalous dimension and $F_I(t)$ is the asymptotic form factor of hadron I. (The non-leading anomalous dimensions are not expected to be given correctly by Eq. (2.3) because of the different weighting of the x_i integrations.) The anomalous logarithms from each wavefunction is specific to each hadron, and thus gives a factorization theorem Eq. (2.1) for the logarithmic corrections to dimensional counting analogous to the factorization theorems for scale-violations to high p_T inclusive reactions.

B. Soft Subprocesses[16]

As first emphasized by Landshoff,[41] amplitudes with "pinch" singularities, analogous to Glauber scattering amplitudes may provide

an alternative and possibly phenomenologically important source of hadrons at large p_T. The classic example is pp scattering, which can proceed via three successive (nearly on-shell) $qq \to qq$ elastic collisions each at $\theta_i \sim \theta_{cm}$ (see Fig. 23). The hadronic amplitude has the form ($\hat{s} \sim 1/3s$, $\hat{t} \sim 1/3t$)

$$\mathcal{M}_{pp \to pp} \sim \left[\frac{i}{\sqrt{stu\lambda^2}}\right]^2 \left[\mathcal{M}_{qq \to qq}\ (\hat{s},\hat{t})\right]^3 \qquad (6.4)$$

which gives nominally for spin 1 exchange

$$\frac{d\sigma}{dt}\ (pp \to pp) \ \sim\ \frac{1}{\lambda^4 t^8}\ f(s/t) \ \sim\ \frac{1}{t^8} \text{ for } s >> t \qquad (6.5)$$

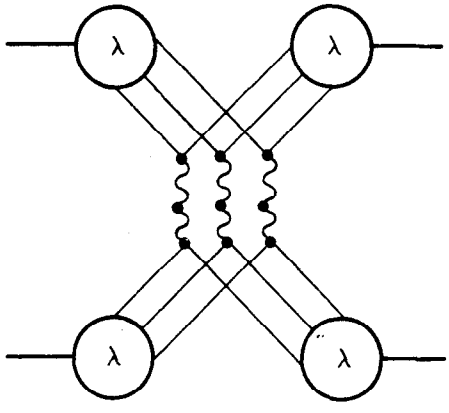

Fig. 23. Landshoff pinch singularity contribution to elastic pp scattering. The elastic $qq \to qq$ amplitudes are nearly on-shell.

The $i/\sqrt{stu\lambda^2}$ factor in Eq. (6.4) represents the probability amplitude for the scattered quarks to overlap with the final state hadrons. As noted by Donnachie and Landshoff,[42] data from the ISR and FNAL at $s > 800$ GeV^2, $4 < |t| < 10$ GeV^2 is compatible with Eq. (6.5). (See Fig. 24.)

The anomalous power law of the pinch singularities arises from exclusive $qq \to qq$ amplitudes where each intermediate state is nearly on-shell. Thus Fock state amplitudes Ψ_λ in the soft domain are required. Since gluon radiation is excluded in this exclusive reaction, $\mathcal{M}_{qq \to qq}$ is suppressed by the Sudakov quark form factor:

$$\mathcal{M}_{qq \to qq} \ \sim \mathcal{M}_{Born} \cdot \alpha_s(\hat{t})\ F_q^2(\hat{t}) \qquad (6.6)$$

The amplitude $F_q(t)$ can be computed from virtual gluon corrections,[43] or more simply from the exclusive-inclusive connection with the $G_{q/q}(x,q^2)$ distribution $P(\tilde{\xi})(1-x)^{\tilde{\xi}-1}$

$$F_q^2(\hat{t}) \ \sim\ [\lambda^2/\hat{t}]^{\tilde{\xi}}\ P(\tilde{\xi}) \qquad (6.7)$$

where

$$\tilde{\xi} = \tilde{\xi}(\hat{t},\lambda^2) = \frac{C_F}{\pi}\int_{\lambda^2}^{\hat{t}} \frac{d\ell^2}{\ell^2}\,\alpha_s(\ell^2) \quad . \tag{6.8}$$

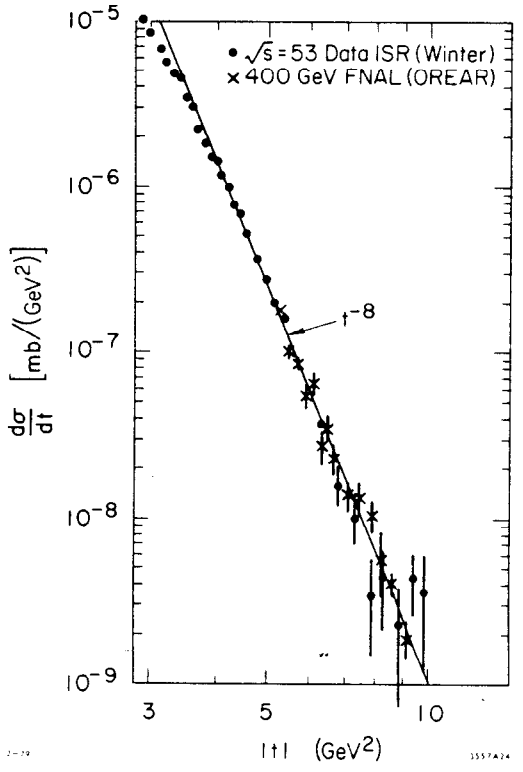

Fig. 24. Comparison of ISR and FNAL data at $s >> |t|$ with the prediction (6.5). (From Ref. 42.)

Thus the leading pinch singularity contribution to pp-scattering falls as

$$\frac{d\sigma}{dt}(pp \to pp) \sim \frac{\alpha_s^6(\hat{t})}{\hat{t}^{8+6\tilde{\xi}}} P^6(\tilde{\xi}) f(s/t) \tag{6.9}$$

where $\tilde{\xi} \sim O(\log\log|\hat{t}|)$. Thus, asymptotically, the pinch contribution falls faster than any power and eventually becomes negligible compared to the hard scattering contributions. Nevertheless, it is possible that such multiple scattering processes do play an important role in the $s >> |t|$ domain of Fig. 24 especially considering the fact that $\hat{t} \sim 1/9t$ is of order ~ 1 GeV^2. However, it is not clear why the ISR and FNAL data do not indicate a faster fall-off than t^{-8} considering the strong variation of $\alpha_s(\tilde{t})$ and non-zero value of $\tilde{\xi}$ in Eq. (6.9).

7. The Phenomenology of pp Scattering at Large Angles

The overall features of $d\sigma/dt\,(pp \to pp)$ are sketched schematically in Fig. 25. The data at central angles $30^\circ \lesssim \theta_{cm} \lesssim 150^\circ$ fall rather uniformly as $s^{-10} f(\theta_{cm})$ and merges with at t^{-8} energy-independent "envelope" in the small θ_{cm} $s >> |t|$ region. This s-independent small θ_{cm} envelope is consistent with multiple gluon exchange mechanisms which produce fixed $J = 1$ Regge behavior. The overall behavior of the central angle data is consistent with the quark

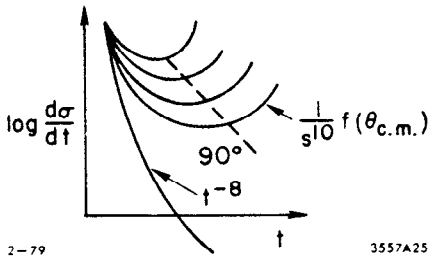

Fig. 25. Qualitative features of elastic pp scattering.

interchange[40] QCD diagrams; the observed shape of $f(\theta_{cm}) \sim (\sin\theta_{cm})^{-10}$ to -14 is compatible with this ansatz. Furthermore, the roughly symmetrical shape of $d\sigma/dt$ $(np \to np)$ around 90° and the large $pp/p\bar{p}$ ratio at 90° are all consistent with quark exchange or interchange hard scattering mechanisms.[40]

However, these mechanisms fail to account for either:

(a) the slow oscillation of the 90° cross section about the s^{-10} prediction (see Fig. 7), nor

(b) the striking, strongly varying spin correlation recently measured by A. Krisch and collaborators at Argonne.[14] (See Fig. 26.) At $s = 24$ GeV^2, $\theta_{cm} = 90°$, it is ~4 times more likely for two protons to scatter with their spins aligned normal and parallel to the scattering plane than anti-parallel. In contrast, the quark interchange amplitude predicts this ratio should be close to 2 independent of angle.[44,45]

The possibility that non-perturbative (instanton) effects could be interfering with the quark interchange amplitude to produce large spin correlations has been investigated by Farrar, Gottlieb, Sivers, and Thomas.[45] More recently Brodsky, Carlson, and Lipkin[44] have considered another possibility: since the triple scattering pinch singularity contribution to pp scattering requires the $qq \to qq$ amplitude at $\hat{s} = 1/9s$ and the relatively low momentum transfer $\hat{t} \sim 1/9t \sim -1.1$ GeV^2, it is not unlikely that the qq scattering is dominated here by simple meson exchange or Reggeon diagrams. In fact a low energy pinch contribution computed with triple "σ" or "π" exchange, interfering with the quark interchange amplitude can

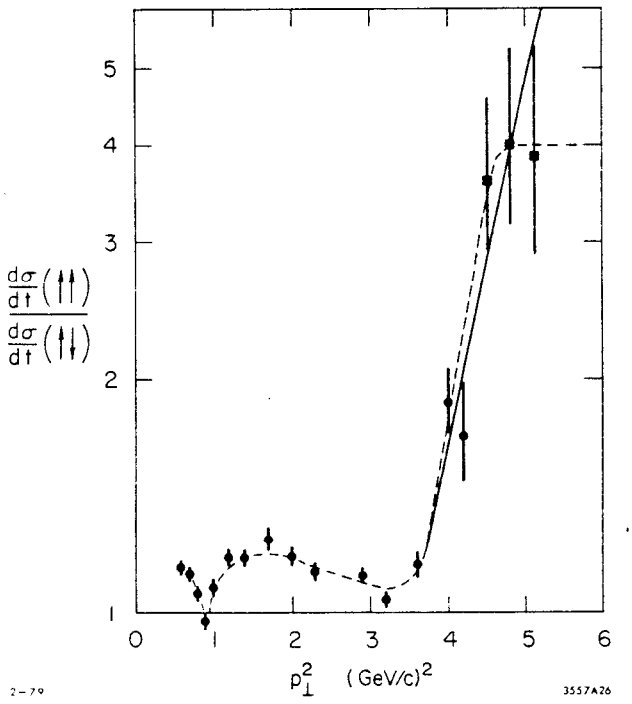

Fig. 26. Spin correlation for protons polarized normal to the scattering plane. (From Ref. 14.)

produce a spin-correlation with the observed magnitude and dependence on θ_{cm}. This model leads to a number of testable predictions including s-dependence, np/pp ratios, and the spin correlation for longitudinally polarized nucleons. A large double-helicity flip amplitude is predicted due to scalar and the pseudoscalar meson exchange.

8. Transverse Momentum Distributions and Inclusive Reactions

It is straightforward to extend the methods discussed here to calculate the $x \to 1$ and large $k_\perp$ behavior of each Fock component of hadronic wavefunctions. In general, one starts with the soft wavefunction $\Psi_\lambda(x,\vec{k}_\perp^2)$ and then uses the evolution equations to obtain the leading power-law and α_s dependence in the far-off-shell domain. In the case of the $q\bar{q}$ component of the (helicity zero) meson wavefunction, the asymptotic fall-off in $\vec{k}_\perp^2$ is given by

$$\psi(\vec{k}_\perp,x)/16\pi^2 \equiv \frac{\partial}{\partial \vec{k}_\perp^2}\tilde{\phi}(x,\vec{k}_\perp^2) \tag{8.1}$$

$$\to \frac{3}{4}k_\pi \frac{1-x^2}{\vec{k}_\perp^2}\frac{C_F}{\beta}\alpha_s(\vec{k}_\perp^2)\cdot\left[\frac{\alpha_s(\vec{k}_\perp^2)}{\alpha_s(\lambda^2)}\right]^{-C_F/\beta}$$

where $k_\pi = f_\pi/\sqrt{n_c}$ in the case of pions. Thus the fall-off in the intrinsic wavefunction is slightly stronger than an inverse power of $\vec{k}_\perp^2$ due to the internal hard gluon interactions, and much slower than the exponential or Gaussian forms usually assumed. The dependence on λ^2 cancels in physical cross sections. This independence in the choice of λ^2 can be used to derive renormalization-group type equations.

The fact that the "tail" of the hadronic wavefunction can be computed at short distances removes the central uncertainty in the calculation of effects due to intrinsic transverse momentum fluctuations for reactions such as massive lepton pair production or high p_T hadronic processes - the hadronic wavefunction is no longer a "black box"! Since the wavefunction enters squared in the inclusive cross sections the spectator transverse momentum integrations are always convergent at large $\vec{k}_\perp^2$. This is in contrast to the $d\vec{k}_\perp^2/\vec{k}_\perp^2\ \alpha_s(\vec{k}_\perp^2)$ integrations from gluon bremsstrahlung which lead to the scale-violations in the input structure functions.

The general analysis of large p_T inclusive reactions in QCD is complicated, but the asymptotic scaling behavior of the inclusive cross section to leading order in $\alpha_s(p_T^2)$ appears to be a tractable problem. Let us consider a given reaction $A+B \to C+X$ where C is detected at large CM angles with transverse momentum p_T and momentum fraction $x_R = |\vec{p}|/p_{max}$. Each hadron A,B, and C is represented by its Fock state components Ψ_λ.

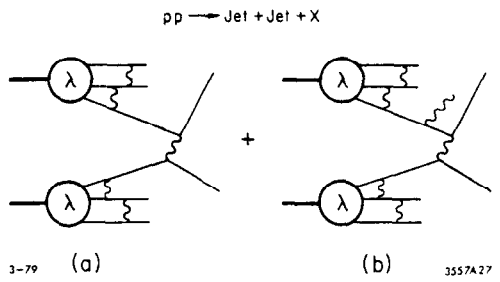

Fig. 27. Example of diagrams which contribute to high p_T pp + jet + X reactions.

We then identify[46] all hard scattering processes T_B (a+b → c+d) which can contribute to the final state high p_T trigger by the scattering of incident constituents (see Fig. 27a). The simplest subprocesses are qq → qq, qg → qg, gg → gg, etc., but for some kinematic regions we should also consider "high twist" subprocesses such as $q\bar{q} \to M\bar{M}$, Mq → Mq, Bq → Bq, etc. As in exclusive scattering, the nominal power-law fall off of T_B in p_T^2 reflects the number (n_{active}) of fundamental fields forced to change directions. By definition every intermediate state associated with T_B and its radiative corrections is off shell by at least λ^2; otherwise its contribution is already included in Ψ_λ.

Furthermore, as $x_R \to 1$, each constituent a,b,c (assuming $c \neq C$) requires the far-off-shell behavior of the Fock state wavefunctions for A,B,C. The leading power law behavior as $(1-x_R) \to 0$ is given by diagrams with the minimal number of gluons exchanged between the Fock state constituents which can transfer all of the hadronic momentum to the hard scattering subprocess. The evolution equations for the Fock state wavefunctions then gives anomalous logarithms $a_i[\alpha_s(k^2_{x_i})]^{\gamma_i}$ where $k^2_{x_i} = -(\vec{k}^2_{T_i} + \tilde{m}^2_i)/(1-x_i)$, as in the structure function calculations. Combining these factors we obtain at large p_T and $x_R \sim 1$

$$E\frac{d\sigma}{d^3p}(A+B \to C+X) \sim \left[\frac{\alpha_s(p_T^2)}{p_T^2}\right]^{n_{active}-2} \cdot (1-x_R)^{2n_s-1}\left[\alpha_s(k^2_{x_R})\right]^{2n_s+\Gamma} f(\theta_{cm}) \tag{8.2}$$

where n_s is the total number of spectators in A,B and C and Γ is the sum of the leading anomalous dimensions for the corresponding Fock states. (The spin complication noted in Section 5 will for simplicity be ignored here.)

Now let us consider the effects of gluon bremsstrahlung for the external lines a,b, and c of T_B, as in Fig. 27b. Taking into account the off-shell kinematics, the integration over gluon transverse momentum up to p_T^2 gives the additional factors

$$\prod_{i=a,b,c} (1-x_i)^{\xi_i(p_T^2,\, k_{x_i}^2)} P(\xi_i) \tag{8.3}$$

which can be incorporated into the structure functions $G_{a/A}(x_a, p_T^2)$, etc. Here

$$\xi_i = \frac{C_i}{\pi} \int_{k_{x_i}^2}^{p_T^2} \frac{d\ell^2}{\ell^2} \alpha_s(\ell^2) \tag{8.4}$$

where C_i is the color SU(3) Casmir operator for a,b or c:

$$C_i = \begin{cases} 0 & \text{color singlets} \\ 4/3 & 3 \text{ or } \bar{3} \\ 3 & \text{octet} \end{cases} \tag{8.5}$$

It is a striking fact that the scale-breaking corrections due to gluon bremsstrahlung vanish in the case of color singlets. Thus in the case of higher twist subprocesses such as $(q\bar{q}) + q \to M + q$, the dominant contribution to the $p_T^2 \to \infty$ asymptotic cross section at large x is obtained when the $(q\bar{q})$ system is in a color singlet.[1] In addition, if a,b,c or d is a color singlet composite system, then we also obtain anomalous logarithm factors from the evolution of the hadronic wavefunctions:

$$\prod_{i=a,b,c,d} \left[\sum_n a_n^{(i)} \left(\frac{\log\, p_T^2/\Lambda^2}{\log\, k_x^2/\Lambda^2} \right)^{-\gamma_n^{(i)}} \right] \tag{8.6}$$

In particular, the leading anomalous dimension γ_0 is zero for helicity zero mesons.

Notice that in the exclusive limit, fixed $\mathcal{M}^2 = (1-x_R)p_T^2$, $p_T^2 \to \infty$, we have $\log(k_x^2/\Lambda^2)/\log(p_T^2/\Lambda^2) \to 1$ and $\tilde{\xi} \to 0$; i.e.: because of the off-shell kinematics the anomalous logarithmic corrections to T_B do not appear in the exclusive limit. The asymptotic inclusive cross section in QCD thus takes the factorized form ($\hat{s} = x_a x_b s$, etc.)

$$E \frac{d\sigma}{d^3p} (AB \to CX) = \sum_{ab \to cd} \int_0^1 dx_a\, G_{a/A}(x_a, \xi_a) \int_0^1 dx_b\, G_{b/B}(x_b, \xi_b)$$

$$\int_0^1 \frac{dx_C}{x_C^2} G_{C/c}(x_C, \xi_C) \frac{d\hat{\sigma}}{d\hat{t}} (ab \to cd) \frac{\hat{s}}{\pi} \delta(\hat{s} + \hat{t} + \hat{u}) \tag{8.7}$$

where

$$G_{a/A}(x_a,\xi_a) \sim (1-x_a)^{2n_s^a - 1 + \xi_a(p_T^2, k_{x_a}^2)} P(\xi_a) \qquad (8.8)$$

is the structure function for finding constituent a in A with light-cone momentum fraction x_a. Equation (8.7) holds for subprocess ab → cd where a,b,c,d are each either quarks, gluons, or color singlets. The exclusive cross section $d\hat{\sigma}/d\hat{t}$ (ab → cd) includes the anomalous logarithms from Eq. (8.6) in the case of composite color singlets. [We have not considered the contribution of multiparticle scattering (pinch singularities) to the inclusive cross sections.] The fact that $\xi_a = 0$ for color singlets implies that structure functions obtained from higher Fock state components such as $G_{M/B}(x,\xi)$ are actually scale-invariant. It thus should be possible to obtain the normalization of these contributions from conventional Deck or Drell (meson-exchange) analyses of multiparticle exclusive processes.

Equation (8.7) is consistent with the usual factorization theorems for inclusive reactions, but it includes the effects of higher twist processes, off-shell effects, and predicts the $(1-x_R) \to 0$ behavior of the cross section. Aside from the computable logarithm corrections, the inclusive cross section is well characterized by the power-law formula (8.2). Since $\xi \to 0$ at $p_T^2 \to \infty$ and fixed $(1-x)p_T^2$, there is again a smooth connection with exclusive processes, and the spectator power law[3] $(1-x_R)^{2n_s-1}$ becomes precise in this limit.

Equation (8.7) is evaluated to leading order in $\alpha_s(p_T^2)$ and includes the effects of the k_T fluctuation due to both gluon radiation and the fall-off of the intrinsic wavefunction. Non-leading terms in m^2/p_T^2 and λ^2/p_T^2 are also obtained from the mass connection to T_B and the soft-wavefunction. Note that the Feynman amplitude qq → qqg contributes to both the qq → qq and qg → qg subprocesses in T_B, depending on whether the extra gluon's or quark's transverse momentum is integrated over. The region of phase space (as in Fig. 27b) where all three particles emerge at large p_T is of higher order in $\alpha_s(p_T^2)$. The use of the correct off-shell kinematics prevents anomalous or singular contributions from the integration over a gluon or quark pole.[46]

9. High p_T Phenomenology

In general, the inclusive cross section $Ed\sigma/d^3p$ (A+B → C+X) is given by a sum of contributions of the form (8.7). The cross section will be dominated at very high p_T by processes involving the minimum number (4) of active constituents, and it will be dominated at $x_R \to 1$, the edge of phase space, by processes involving the minimum number of Fock state spectators. In addition, for specific trigger particles or systems, specific channels or subprocesses may be anomalously suppressed. The most important effect, often referred to as "trigger bias"[47] greatly suppresses the contribution of processes requiring quark or gluon jet fragmentation.

As an example, consider the inclusive single particle trigger process $pp \to pX$. Hard scattering contributions such as $qq \to qq$ yield cross sections with the asymptotic large p_T, $x_R \to 1$ behavior

$$E\frac{d\sigma}{d^3p}(pp \to pX) \sim \frac{\alpha_s^2(p_T^2)}{p_T^4}(1-x_R)^{11+3\tilde{\xi}}\left[\alpha_s(k_{x_R}^2)\right]^{12+6\gamma_N} \quad (9.1)$$

Although this contribution should eventually dominate at very high p_T, it is suppressed in normalization by several orders of magnitude[47] because of the fact that only a finite fraction of the outgoing quarks momentum is transferred to the proton; the actual hard scattering subprocess thus occurs at a fractionally higher value of p_T where the cross section is much smaller. It is this effect that leads to the prediction of sizeable jet/single ratios in simple QCD subprocesses.[48]

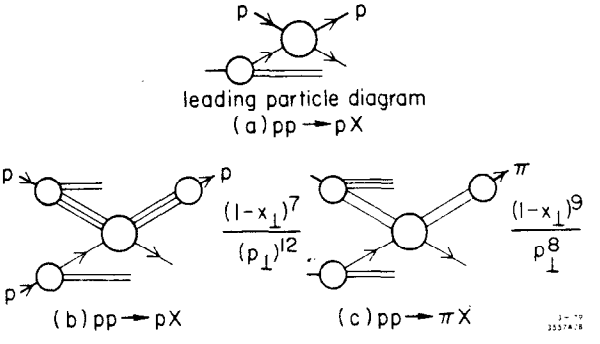

Fig. 28. High twist contributions to high p_T $pp \to pX$ and $pp \to \pi X$ inclusive reactions.

Alternatively we can consider processes where the trigger hadron emerges directly from the hard scattering reaction.[49,50] These are higher "twist" subprocesses in that more than the minimum number of active constituents are involved.

As we have discussed in Section 8, the leading contributions at large x occur when the composite systems are color singlets. The simplest such subprocess is the "leading particle" diagram of Fig. 28a where the hard scattering reaction is $pq \to pq$, i.e.: elastic proton quark scattering. The nominal order is

$$E\frac{d\sigma}{d^3p}(pp \to pX) \sim \frac{[\alpha_s(p_T^2)]^{6+2\gamma_N}}{p_T^{12}}(1-x)^{3+\tilde{\xi}}\,[\alpha_s(k_x^2)]^{4+2\gamma_N} \quad (9.2)$$

Such a contribution is expected to dominate near the exclusive boundary, but is strongly peaked toward forward angles because all of the beam energy is utilized. If we consider a high Fock-state component of the incident nucleon, e.g., $|qqqq\bar{q}\rangle$, then this problem is avoided and one obtains contributions with the form

$$E\frac{d\sigma}{d^3p}(pp\to pX) \sim \frac{[\alpha_s(p_T^2)]^{6+2\gamma_N}}{p_T^{12}}(1-x_R)^{7+\tilde{\xi}}[\alpha_s(k_x^2)]^{8+\Gamma} \quad (9.3)$$

from the B+q → p+q subprocess (see Fig. 28b). Similarly the M+q → πq subprocess (see Fig. 28c) leads to a contribution

$$E\frac{d\sigma}{d^3p}(pp\to \pi X) \sim \frac{\alpha_s^4(p_T^2)}{p_T^8}(1-x_R)^{9+\tilde{\xi}}[\alpha_s(k_x^2)]^{10+\Gamma} \quad (9.4)$$

Since these are the leading QCD contributions which produce hadrons at $\theta_{cm} = 90^o$ directly without the trigger bias suppression, these terms can dominate the inclusive cross section until very large p_T where the nominal p_T^{-4} terms take over.[51] Measurements at FNAL and ISR for pp → pX and pp → πX are in fact consistent with the predicted powers, Eqs. (9.3) and (9.4), respectively for $3 < p_T < 8$ GeV.[52] There are also indications from ISR measurements[53] of pp → π°X, that the fixed x_R power law fall-off changes from p_T^{-8} to $\sim p_T^{-5}$ for $8 \lesssim p_T \lesssim 12$ GeV.

Independent of these phenomenological questions, the important point is that higher twist subprocesses, including the scale-breaking corrections from wave-functions and bremsstrahlung processes (as in Fig. 29) can be systematically computed in QCD. It should also be possible to calculate the normalization of these processes directly from form factor normalizations, and relative normalization of different Fock state components. For example the important $(q\bar{q})+q \to \pi+q$ subprocesses for pp → πX requires the normalization of the $|qqqq\bar{q}\rangle$ Fock state component of the nucleon, which in turn can be computed from the intrinsic sea-quark distribution in the nucleon.

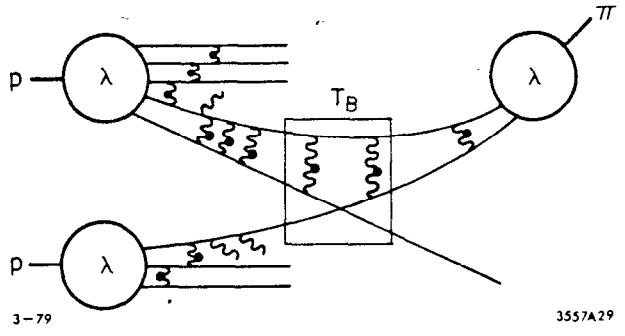

Fig. 29. Example of diagrams which contribute to scale-breaking and anomalous logarithm corrections to the qM → qM higher twist subprocess contribution to pp → πX.

10. Summary

As we have discussed in this paper, the testing ground of quantum chromodynamics can be extended to exclusive processes at large momentum transfer. The essential features which are required in the calculation of the cross sections are (a) the unambiguous separation of hard (far-off-shell) and soft regimes of each hadronic Fock component and (b) the derivation of evolution equations which determine the wavefunctions at short distances. The eigenvalues of the evolution equations yield the anomalous scale-breaking logarithms which are specific to each hadron and systematically correct the leading power behavior of large momentum transfer amplitudes. The dimensional counting rules, modulo calculable logarithmic corrections, thus emerge as predictions of perturbative QCD.

In particular we have obtained

(a) exact results for hadronic form factors at large Q^2 and hadronic structure functions for x near 1,
(b) the asymptotic behavior (including factorization theorems) for fixed angle amplitudes,
(c) the asymptotic suppression of Landshoff (pinch-singularity) contributions for exclusive processes,
(d) a smooth exclusive-inclusive connection in QCD.

The last result depends critically on recognizing the off-shell nature of subprocesses within hadrons, and the fact that the parameter ξ which controls scale-violations in QCD actually vanishes in the fixed $\mathcal{M}^2$, $Q^2 \to \infty$ limit. We have also shown that higher twist and constituent interchange model subprocesses can be systematically computed in QCD.

The Fock space decomposition of the hadronic wavefunctions, together with the axial gauge provides an exact description of QCD which is the analogue of the parton model. In particular it allows us to make a clean distinction between intrinsic sea-quarks and those evolved from the Q^2 dependence of deep inelastic scattering. In general, the lowest particle number Fock states $|B\rangle = |qqq\rangle$ and $M = |q\bar{q}\rangle$ dominate the power law behavior of large momentum transfer exclusive reactions and inclusive reactions at $x \to 1$. The existence of Fock states at $P \to \infty$ with a fixed number of constituents is a consequence of the fact that a hadron is a color singlet.

It is worth emphasizing that QCD predicts specific integral powers for the asymptotic form factors of hadrons:

$$F_\pi(t) \underset{t\to-\infty}{\Longrightarrow} \frac{\alpha_s(t)}{t^1} \quad , \quad F_N^{(1)}(t) \underset{t\to-\infty}{\Longrightarrow} \frac{[\alpha_s(t)]^{2+\gamma_N}}{t^2}$$

Similarly, the asymptotic form of the nucleon structure function is predicted

$$F_{2N}(x,Q^2) \Longrightarrow (1-x)^{3+\tilde{\xi}(Q^2,k_x^2)}$$

The integral powers in these expressions directly test both the scale-invariance of the internal interactions, and the SU(3) color prediction that the minimal Fock states which are color singlets are $|q\bar{q}\rangle$ and $|qqq\rangle$. In this sense, exclusive processes at large momentum transfer and the x near 1 dependence of structure functions provide the most direct and critical prediction of QCD dynamics and color SU(3) symmetry.

At this point, the study of exclusive reactions in QCD is just beginning, but there seems to be real hope that a microscopic description of a large range of hadronic physics will emerge. The anomalous logarithms which emerge from the evolution equation can play a dominant role in phenomenology and may be experimentally accessible from detailed comparisons of different reactions, e.g., $F_\pi(t)/F_K(t)$, meson photoproduction, Compton scattering, etc. The anomalous dimensions are fundamental parameters of each hadron and reflect the underlying symmetry properties of its wavefunction. In some cases the absolute normalization of amplitudes such as the meson form factors, $\gamma(q^2) + \gamma(k^2) \to \pi^o$ can be computed in the asymptotic limit. It also should be possible to compute the normalization of large angle scattering processes and higher twist (CIM) subprocesses in terms of the normalization of the meson and baryon form factors as well as their angular distributions. We are also analyzing the spin structure of baryon wavefunctions in the short distance limit. In principle, it should be possible to make a direct connection between the soft Fock space wavefunctions Ψ_λ and the wavefunctions used in hadronic spectroscopy, bag models, etc. The higher Fock state components also evidentally play an important role in the sea quark distribution, low momentum hadron exchange reactions, and inclusive reactions in the fast ($x_L \to 1$) forward regime.[3]

Acknowledgements

We wish to thank our collaborators, Y. Frishman and C. Sachrajda for many discussions. We also thank R. Blankenbecler, G. Farrar, J. Gunion, R. Horgan, K. Wilson, and T. M. Yan for helpful conversations.

References

1. S. J. Brodsky and G. R. Farrar, Phys. Rev. Lett. 31, 1153 (1973); Phys. Rev. D11, 1309 (1975).

2. V. A. Matveev, R. M. Muradyan and A. V. Tavkheldize, Lett. Nuovo Cimento 7, 719 (1973).

3. The spectator rule holds for general structure functions $G_{a/A}(x)$ including the case where a is composite. See S. J. Brodsky and R. Blankenbecler, Phys. Rev. D10, 2973 (1974).

4. S. J. Brodsky, in Proceedings of the International Conference on Few Body Problems, Laval University, Quebec (1974), edited by R. Slobodrian et al.

5. S. J. Brodsky and B. Chertok, Phys. Rev. D14, 3003 (1976); Phys. Rev. Lett. 37, 269 (1976).

6. M. D. Mestayer, SLAC-Report No. 214 (1978).

7. R. Arnold et al., Phys. Rev. Lett. 35, 776 (1975).

8. R. Anderson et al., Phys. Rev. Lett. 30, 627 (1973).

9. M. A. Shupe et al., Tufts, Harvard, Cornell collaboration (to be published).

10. K. A. Jenkins et al., Phys. Rev. Lett. 40, 425 (1978).

11. P. V. Landshoff and J. C. Polkinghorne, Phys. Lett. 44B, 293 (1973).

12. J. L. Stone et al., Phys. Rev. Lett. 38, 1315 (1978); Nucl. Phys. B143, 1 (1978).

13. A. Hendry, Phys. Rev. D10, 2300 (1974).

14. D. G. Crabb et al., Phys. Rev. Lett. 41, 1257 (1978).

15. G. P. Lepage and S. J. Brodsky (in preparation). A preliminary report of this work is given in S. J. Brodsky, SLAC-PUB-2240 (December 1978), to be published in the Proceedings of the J. H. Weis Memorial Symposium on Strong Interactions (November 1978).

16. S. J. Brodsky, G. P. Lepage, Y. Frishman and C. Sachrajda (in preparation).

17. D. R. Jackson, Ph.D. Thesis, Cal Tech (1977). G. R. Farrar and D. R. Jackson (to be published).

18. A. V. Efremov and A. V. Radyushkin, paper submitted to the XIX International Conference on High Energy Physics (Tokyo, 1978) and to the International Seminar on High Energy Physics and Field Theory (Serpurkhov, July 1978). Note added: After our work was completed we received Dubna preprint E2-11983 in which Eq. (2.1) is also derived by these authors.

19. A. M. Polyakov, reporteur's talk, Lepton-Photon Symposium, SLAC (1975).

20. P. Menotti, Phys. Rev. D14, 3560 (1976); Phys. Rev. D11, 2828 (1975).

21. T. Appelquist and E. Poggio, Phys. Rev. D10, 3280 (1970).

22. M. L. Goldberger, A. H. Guth, D. E. Soper, Phys. Rev. D14, 1117 (1976).

23. M. Einhorn, Phys. Rev. D14, 3451 (1976); R. C. Brower, J. Ellis, M. G. Schmidt and J. H. Weis, Nucl. Phys. B128, 131 (1977); Phys. Lett. 65B, 249 (1976).

24. See S. Weinberg, Phys. Rev. 150, 1313 (1966); L. Susskind and G. Frye, Phys. Rev. 165, 1535 (1968); J. B. Kogut and D. E. Soper, Phys. Rev. D1, 2901 (1970); J. D. Bjorken, J. B. Kogut and D. E. Soper, Phys. Rev. D3, 1382 (1971). Renormalization theory is implemented in this framework by S. J. Brodsky, R. Roskies and R. Suaya, Phys. Rev. D8, 4575 (1978); and W. Caswell and G. P. Lepage, Phys. Rev. A18, 810 (1978) for the case of bound states.

25. We wish to thank R. P. Feynman for an illuminating discussion on this point.

26. W. Caswell and G. P. Lepage, Ref. 24.

27. S. J. Brodsky, R. Roskies and R. Suaya, Ref. 24.

28. See, e.g., G. Alterelli and G. Parisi, Nucl. Phys. B126, 298 (1977). For an excellent review see C. H. Llewellyn Smith, Acta. Physica Austriaca Suppl. XIX, 331-397 (1978).

29. Yu. L. Dokshitser, D. I. D'Yakanov and S. I. Troyan, SLAC-TRANS-183 (translation for Proceedings of the 13th Leningrad Winter School on Elementary Particle Physics (1978)).

30. See, e.g., D. J. Gross and S. B. Trieman, Phys. Rev. Lett. 32, 1145 (1974); and R. Coquereaux et al., Ref. 43.

31. H. D. Politzer, Phys. Rev. Lett. 30, 1346 (1976); and Phys. Reports 14, 129 (1974).

32. D. J. Gross and F. Wilczek, Phys. Rev. Lett. 30, 1323 (1973); Phys. Rev. D8, 3633 (1973); and Phys. Rev. D9, 980 (1974).

33. S. J. Brodsky and J. F. Gunion, Phys. Rev. D19, 1005 (1979).

34. G. R. Farrar, Nucl. Phys. B77, 429 (1974); J. F. Gunion, Phys. Rev. D15, 3317 (1977), and D10, 242 (1974).

35. Z. F. Ezawa, Nuovo Cimento 23A, 271 (1974).

36. G. R. Farrar and D. R. Jackson, Phys. Rev. Lett. 35, 1416 (1975).

37. A. I. Vainshtain and V. I. Zakharov, Phys. Rev. Lett. 72B, 368 (1978).

38. E. L. Berger and S. J. Brodsky, SLAC-PUB-2247 (1979), to be published in Phys. Rev. Lett.

39. K. J. Anderson et al., Chicago-Princeton Report EFI-78-38.

40. R. Blankenbecler, S. J. Brodsky and J. F. Gunion, Phys. Rev. D8, 4117 (1973); Phys. Lett. 39B, 649 (1972).

41. P. V. Landshoff, Phys. Rev. D10, 1024 (1974). See also P. Cvitanovic, Phys. Rev. D10, 338 (1974); and S. J. Brodsky and G. Farrar, Ref. 1.

42. A. Donnachie and P. V. Landshoff, Preprint M/C 79/11 (January 1979).

43. This work on the asymptotic suppression of pinch singularities in QCD was done in collaboration with Y. Frishman.[16] The quark form factor in QCD is discussed by J. Cornwall and G. Tiktopolus, Phys. Rev. D13, 3370 (1976) and D15, 2937 (1977); R. Coquereaux and E. DeRafael, Phys. Lett. 74B, 135 (1978); and E. C. Poggio and H. R. Quinn, Phys. Rev. D12, 3279 (1975).

44. S. J. Brodsky, C. Carlson and H. Lipkin, SLAC-PUB (in preparation).

45. G. R. Farrar, S. Gottlieb, D. Sivers and G. H. Thomas, ANL preprint HEP-PR-78-43 (1978).

46. See S. J. Brodsky, R. R. Horgan and W. E. Caswell, Phys. Rev. D18, 2415 (1978).

47. S. D. Ellis, P. V. Landshoff and M. Jacob, Nucl. Phys. B108, 93 (1978); and P. V. Landshoff and M. Jacob, Nucl. Phys. B113, 395 (1976).

48. See, e.g., R. Field, R. P. Feynman and G. C. Fox, Phys. Rev. D18, 3320 (1978) and references therein.

49. R. Blankenbecler, S. J. Brodsky and J. F. Gunion, Phys. Rev. D18, 900 (1978) and references therein.

50. P. V. Landshoff and J. C. Polkinghorne, Phys. Rev. D10, 891 (1974) and references therein; M. K. Chase and W. J. Stirling, Nucl. Phys. B133, 157 (1978).

51. For a comprehensive discussion see D. Jones and J. F. Gunion, Phys. Rev. D19, 1032 (1979).

52. D. Antreasyan et al., Phys. Rev. D19, 764 (1979) and references therein.

53. For a recent review see M. Jacob and P. V. Landshoff, Phys. Report 48, 285 (1978). For $7.5 < p_T < 14.0$ GeV/c, $\sqrt{s} = 53.1$ and 62.4 GeV, a good fit to the ISR-CCOR data is obtained with $Ed\sigma/d^3p\ (pp \to \pi^o X) = p_T^{-5.1 \pm 0.4} f(x_T)$; CCOR collaboration, Phys. Lett. 79B, 505 (1978).